Plasma Science and Technology

PAPER

Development of a portable cold air plasma jet device and observation of its photo ionization process

Plasma Sci. Technol. **22** (2020) 085403 (10pp) https://doi.org/10.1088/2058-6272/ab8d1b

Development of a portable cold air plasma jet device and observation of its photo ionization process

Zhaoquan CHEN (陈兆权), **Jinfang WU** (吴金芳), **Huang ZHANG** (张煌), **Ming ZHANG** (张明), **Sanyang ZHANG** (张三阳) **and Deren FENG** (冯德仁)

Anhui Key Laboratory of Electrical Drive and Power Electronics, Anhui University of Technology, Maanshan 243032, People's Republic of China

E-mail: chenzq@ahut.edu.cn

Received 12 March 2020, revised 25 April 2020
Accepted for publication 26 April 2020
Published 5 June 2020

Abstract

Photo ionization plays a critical role in the formation and propagation of atmospheric pressure plasma jet plumes. But in experiments, it is very difficult to observe the photo ionization due to its relative lower density of photo electrons. In the present study, we develop a portable cold air plasma jet device and observe the ionization wave in a dc spark air plasma jet. The discharge images acquired by an ICCD camera show that the ionization wave front performs as a quickly moving bright ball. Breakdown could take place at another side of the quartz plate or pork tissue layer (6 mm thick), which suggests that the ionization should be attributed to photo ionization. The laser schlieren images indicate there is propagation of a shock wave along with the plasma bullet. Based on the photo ionization theory and the photo-electric measurement, the direct photo ionization and multistage photo ionization are the main factors in charge of generating the cold air plasma jet. In addition, the plasma jet outside of the cathode nozzle is colder than 320 K and can be touched safely by a human. In view of the plasma jet including a large amount of active particles, such as NO, O, OH, emitted photons, etc, the proposed portable cold air plasma jet device could be qualified for plasma bio-medicine applications.

Keywords: photo ionization, air plasma jet, plasma bullet, ionization wave

(Some figures may appear in colour only in the online journal)

1. Introduction

Atmospheric pressure plasma jets (APPJs) are generated in ambient air rather than in a limited space, which is more suitable for applications in materials surface modification, ignition or combustion, and plasma bio-medicine [1–3]. Different applications require the applied APPJs with specific parameters. For plasma medicine, the APPJ needs to satisfy some strict restrictions, for example no hot stimulation, no electrical shock, portable, reuse, lower cost, etc. Recently, most APPJs apply Ar or He as the working gas; this confers the APPJs' device unavoidably with a heavy and complex gas supply equipment [4–6]. Therefore, the best choice for the working gas is to use ambient air directly.

Focusing on portable air APPJs, there are three kinds of air plasma jet developed for biomedical applications, such as self pulsed dc driven air plasma [7–10], floating electrode kHz dielectric barrier discharge (DBD) air plasma [11, 12] and microwave air plasma jet [13]. Apart from the only weakness of low-frequency air plasma devices (pulsed dc or kHz) suffering from high amounts of ozone and microwave air plasma working with the special supply of air flow (complex in microwave generating and plasma control), these three typical air plasma devices [7–13] all have excellent performances. In recent research, Dobrynin D *et al* [14, 15] have reported an advanced air plasma jet (mainly with NO but with little ozone) generated by a pin-to-hole spark discharge (PHD) device. However, due to it having a bigger capacitance

and thereafter higher discharge intensity, the PHD air plasma has significant UV radiation and hydrogen peroxide. In order to decrease the temperature of the plasma jet plume, air flow is applied. In addition, a 4–8 kV high-voltage power supply and 0.33 μF larger volume capacitor make it too heavy to be portable. Therefore, a portable air plasma device without ozone but with intense NO is still worth exploiting.

For air discharge at atmospheric pressure, the PHD works in cathode-directed streamers [14, 15]. Most APPJs perform as the bullet-like lightened volume (plasma bullet or guided ionization wave front) moves at the speed of 10^2–10^6 ms^{-1} to compose the plasma jet [1–5]. For the propagation of the plasma bullet, seed electrons ahead of the guided ionization wave front are necessary, and these seed electrons can be originated from ionization of natural radioactivity, residual electrons left from previous discharge, O_2^- detachment and photo ionization [2]. As we know, the seed electron density due to natural radioactivity ionization is very low (about 10^4 cm^{-3} in ambient air); O_2^- detachment is mainly determined by the high electric fields and the gas temperature; and the density of leftover free electrons from previous pulses for the pulse frequency at both 400 Hz and 250 Hz are much lower than 10^6 cm^{-3} [2]. Thus, the seed electrons induced by photo ionization play a critical role in guiding the streamer propagation in APPJs. Especially, when photo ionization effect is taken part in a simulated model, the electron cloud with the density of 10^6–10^8 cm^{-3} has been taking place at the surrounding domain of the ionization wave front [16–18].

In order to check the effect of photo ionization on the streamer front propagation, Wu *et al* [19] have designed a special experiment that records the optical emission spectra; the detected results are verified by theoretical predictions that indicate that 98–102.5 nm VUV photons radiated by excited N_2 can ionize O_2 directly. However, in their experiment, no direct evidence suggests whether the emitted photons around the streamer front are generated by photo ionization or not. The main factor is due to the fact that for repetitive kHz APPJs, the density of residual electrons left from previous pulses might be much higher than the seed electrons produced by photo ionization. Therefore, it should be possible to decrease the driven pulse frequency to lower than 100 Hz to make sure the residual electrons left from previous discharge have been decreased to the intensity less than 10^5 cm^{-3}. In other words, it is necessary to verify that the seed electrons in charge of guiding the plasma bullet propagation in the PHD air plasma jet plume should be mainly generated by photo ionization. Therefore, the purposes of the present study mainly focus on the observation of photo ionization in a dc spark plasma jet generated by a portable cold air plasma device.

2. Experimental setup and operations

Figure 1 shows the cold air plasma jet plume generated by dc spark discharge. A 3.7 V rechargeable lithium ion battery with a charge capacity of 1.2 Ah is connected with a 4 kV dc power module. The output port of the 4 kV dc power module (the maximum dc voltage of 5000 V can be excited) is in parallel connection with a 47 nF capacitor (to withstand high voltage of 6 kV) and a PHD device. The PHD device consists of a pin-shaped anode (30 mm long, 2 mm in diameter and a sharpened end), ceramic tube (30 mm long, inner diameter of 2 mm and outer diameter of 4 mm), and a tube-shaped cathode (20 mm long, inner diameter of 4 mm and outer diameter of 6 mm) with a hole nozzle (central hole with diameter of 2 mm). Both electrodes are made of stainless steel. As shown in figure 1(a), when the switch is on, the capacitor will be charged slowly to high voltage and the spark discharge can be generated by the PHD device. In order to make sure the air plasma jet can stretch out to a longer distance, a 1 mm air gap between the end of the ceramic tube and the hole nozzle is set; another 1 mm air gap in the ceramic tube is arranged near the end of the sharp pin.

Figure 1(b) shows the working process during a discharge period. When the output voltage of the capacitor reaches about 4200 V, the spark discharge takes place in the air gap. In the time scale of tens of nanoseconds, the main discharge is completed and the capacitor results in a voltage drop. This is step 1. The discharge is moving forward in step 2. In step 2, the connected line is with parasitic inductance L and the PHD device (plasma channel can be treated simply as a resistance R_p) is parallel connected with the capacitor C to constitute a LCR series resonant circuit. Then the air around the discharge channel is heated to very hot in the time scale of hundreds of nanoseconds, the air gas pressure grows up in an instant, and that will further result in air plasma blowouts to form an air plasma jet. Although the air plasma in the air gap is very hot, the temperature of the plasma jet out of the nozzle is near to room temperature, due to the gas blowout effect [14]. The LCR oscillation is ended after tens of microseconds, the air in the air gap is cooled after hundreds of microseconds, and then the air gas pressure in the air gap becomes less than atmospheric gas pressure. Hence, air recovery happens in step 3 during a timescale of tens of milliseconds. Thereafter, the next discharge happens as the voltage of the capacitor again gets up to 4200 V.

Figure 1(c) shows a portable air plasma device. The device has a length of 12 cm, width of 5 cm, and thickness of 3 cm. The total weight is about 120 g. It has a switch button to turn on or off. A charging port can be used to charge the lithium ion battery, which shares the same charger as a mobile phone. It can be used to cure beriberi, wound hemostasis, wound and ulcer healing, acne treatment, etc [1–3]. The shock wave caused by spark discharge is too loud (a defect). For decreasing the noise, we designed a rubber cap around the nozzle. In addition, the rubber cap can avoid flowing away the active ingredients of the plasma jet and increase plasma treatment effect. As shown in figure 1(d), the plasma jet with length about 14 mm and diameter about 7 mm is generated in ambient air. It can be held easily and the plasma jet plume can be touched by the human body directly without any feeling of electric shock and hot stimulation, as shown in figure 1(e).

As shown in figure 1(a), the high voltage on the anode of the PHD device is captured by a high-voltage probe (Tektronix P6015A, 1000:1); and the current of the discharge is measured by a current probe (Tektronix TCP 2020). For

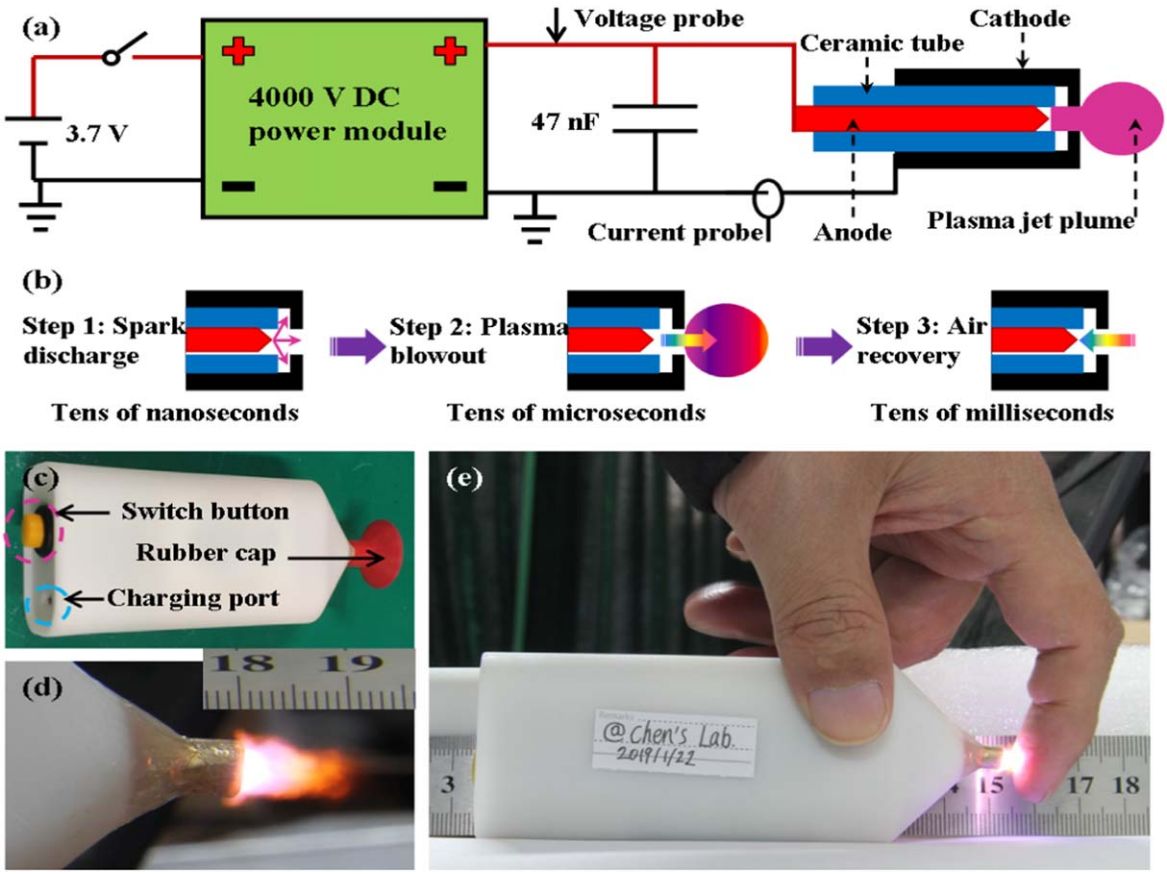

Figure 1. Cold air plasma jet plume generated by dc spark discharge. (a) circuit structure; (b) one working cycle; (c) a portable air plasma device; (d) discharge image of air plasma jet plume; and (e) cold air plasma jet plume touched by human finger.

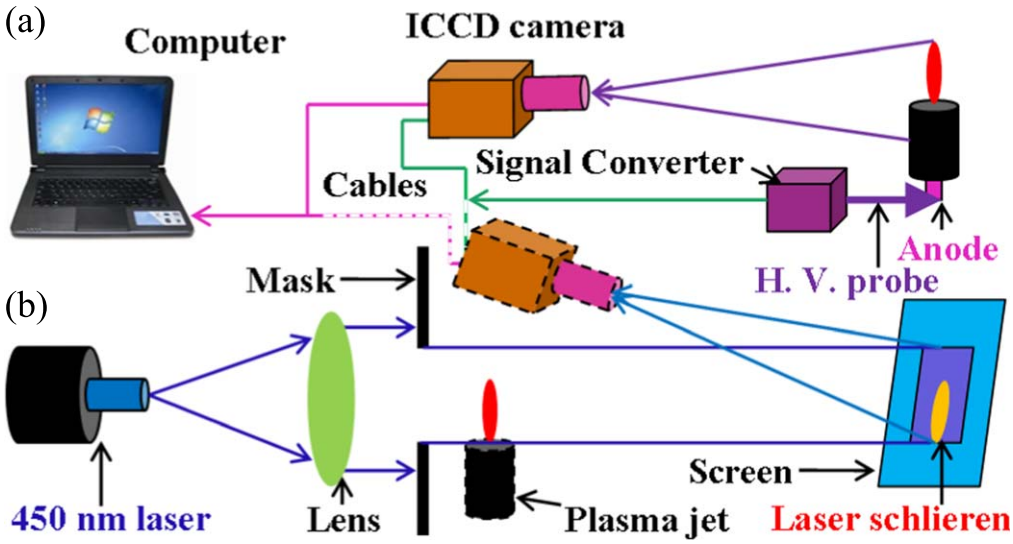

Figure 2. Diagram of the measuring system. Both (a) high-speed discharge image and (b) laser schlieren image are captured by ICCD camera.

taking photos of high-speed images, figure 2 shows a diagram of the measuring system. A fast-gated ICCD camera (Andor, iStar performance sheet DH340T, pixels: 2048 × 512, exposure time: 1.9 ns–10 s, and gains: 0–4450) is applied to capture discharge images [20–23], as shown in figure 2(a). In order to study the shock wave of the spark discharge, a laser schlieren measuring system is formed, as shown in figure 2(b). A square-shaped light beam emitted by a 450 nm laser penetrates the plasma jet and projects it onto a screen. The laser schlieren image can also be captured by the ICCD camera. The ICCD camera is externally triggered by the voltage signal that is converted directly from the measured

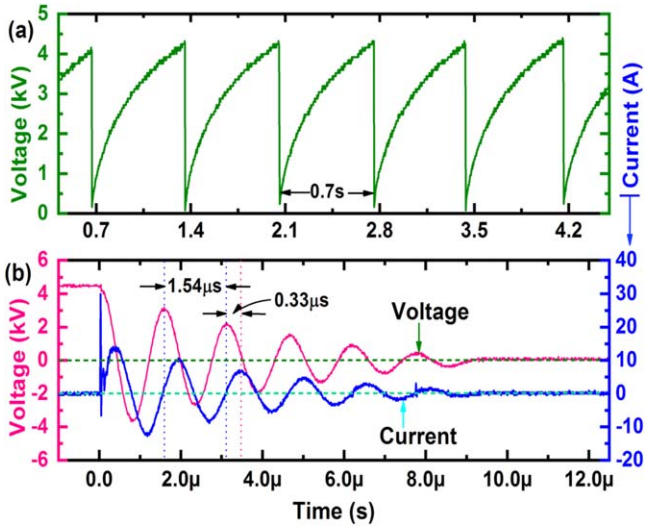

Figure 3. Voltage and current waveform taken from the air discharge experiment. (a) voltage curve displayed in second time scale and (b) voltage and current curves shown in microsecond time scale.

value of the high-voltage probe for synchronizing with the discharge. Moreover, a fiber spectrophotometer (Avantes, AvaSpec 2048) is used to take the spectral line from 200 nm to 1100 nm. For checking the ultra violet spectra, a PI monochromator (Acton SP2500, three grating: 300 l mm^{-1}, 600 l mm^{-1}, and 1200 l mm^{-1}) is applied. The dispersed light emission from the monochromator is detected by a PI-Max 2 ICCD (acting as a spectrometer). The monochromator is calibrated with the spectral line of a mercury lamp [19].

3. Results and discussions

3.1. Electrical and spectral measurements

Figure 3 shows the voltage and current waveform taken from the air spark discharge experiment. As shown in figure 3(a), the high voltage rises up to about 4200 V slowly and then the discharge takes place quickly; the period is about 0.7 s and the discharge has good repeatability, which ensures we can use the falling edge of voltage waveform as the external trigger signal. Figure 3(b) shows the voltage and current curves in microsecond time scale. During the start of tens of nanoseconds, there is a main discharge with the peak value of current up to 30 A, and a voltage drop on the capacitor is steeply about 250 V. After that, the plasma channel is formed. We treat the plasma channel as a resistance R_p simply. In fact, the value of the resistance R_p is varied with time. But here the resistance R_p is simplified as a constant. Therefore the plasma resistance R_p, the capacitor C and the parasitic inductance L of two connected lines are in series and a typical LCR series resonant circuit is formed. The voltage and current waveform shown in figure 3(b) are generated by the LCR circuit oscillation and it evidently belongs to the case of under damped resonance ($R_p{}^2 < 4L/C$). According to circuit theory, there exists a group of formulae, as follows:

$$U_C = U_0 \exp\left(-\frac{t}{\tau}\right)\cos\left(\frac{2\pi}{T}t + \phi_0\right), \tag{1}$$

$$\tau = \frac{2L}{R_p},\ T = \frac{2\pi\sqrt{LC}}{\sqrt{1 - \frac{R_p^2 C}{4L}}}, \tag{2}$$

where U_C is the voltage on the capacitor and U_0 is the started voltage on the capacitor. t is time, τ is the damped factor, and T is the period. As shown in figure 2 (b), the voltage amplitude damped from 4000 V to 1471 V ($U_C = U_0/2.72$) costs about 4.5 μs. Hence, the damped factor τ equals 4.5 μs. The period T is 1.54 μs and the capacitor C equals 47 nF. Taking these numbers into equation (2), $L = 1.276\ \mu$H and $R_p = 0.57\ \Omega$ can be calculated. On the other hand, the parasitic inductance L of two connected lines can be acquired from the line inductive equation,

$$L = \frac{\mu_0 l}{2\pi}\left(\ln\frac{2l}{r} - 0.75\right), \tag{3}$$

where $\mu_0 = 4\pi \times 10^{-7}$ Hm^{-1}, the line length of both connected lines l approximates 0.4 m, and the line radius r is about 4×10^{-4} m. Thence, the parasitic inductance L approximates 1.21 μH, which value is closed to $L =$ 1.276 μH and suggests that the simplified circuit model is well in description. The voltage wave is ahead of the current waveform about 0.33 μs indicating that the LCR series resonant circuit is inductive. During the started main discharge process, the voltage drop on the capacitor is steeply about 250 V and then the energy deposition approximates to 47 mJ. During the following resonant discharge process, the voltage drop on the capacitor is from 4000 V to 0 V in the time of 10 μs and the energy deposition on the R_p of the LCR series circuit is about 376 mJ. Therefore, the electrical energy absorbed by plasma is mainly through Ohmic heating (the current heats the plasma channel and the total energy deposition per pulse is about 420 mJ).

Next, we will continue to check what active components are included in the plasma jet by spectral measurement. Figure 4(a) shows the spectra detected by the fiber spectrophotometer. It is clearly shown that the proposed plasma jet contains a large amount of active particles, such as NO, O, OH, emitted photons, etc. We have known that NO has an anti-inflammatory effect, O and OH are highly oxidant particles, and ultra violet radiation is capable of sterilizing and diminishing inflammation [1–3, 24]. Furthermore, in order to verify the theoretical prediction of photo ionization in air gas (the wavelength shorter than 102.5 nm VUV photons can ionize O_2 directly [25–27]), we should check whether there are 98–102.5 nm VUV photons radiated by excited N_2 or not. However, due to the fact that the brand of optical fiber probe that passes radiation of spectra is from 190 nm to 1100 nm, we cannot capture the spectra of 98–102.5 nm. Figure 4(b) shows the VUV spectrum that is from 165 nm to 235 nm. Here, the optical fiber probe is located in the plasma jet plume and the probe hole is aligned with the central axis of the discharge nozzle (2 mm away from the cathode end).

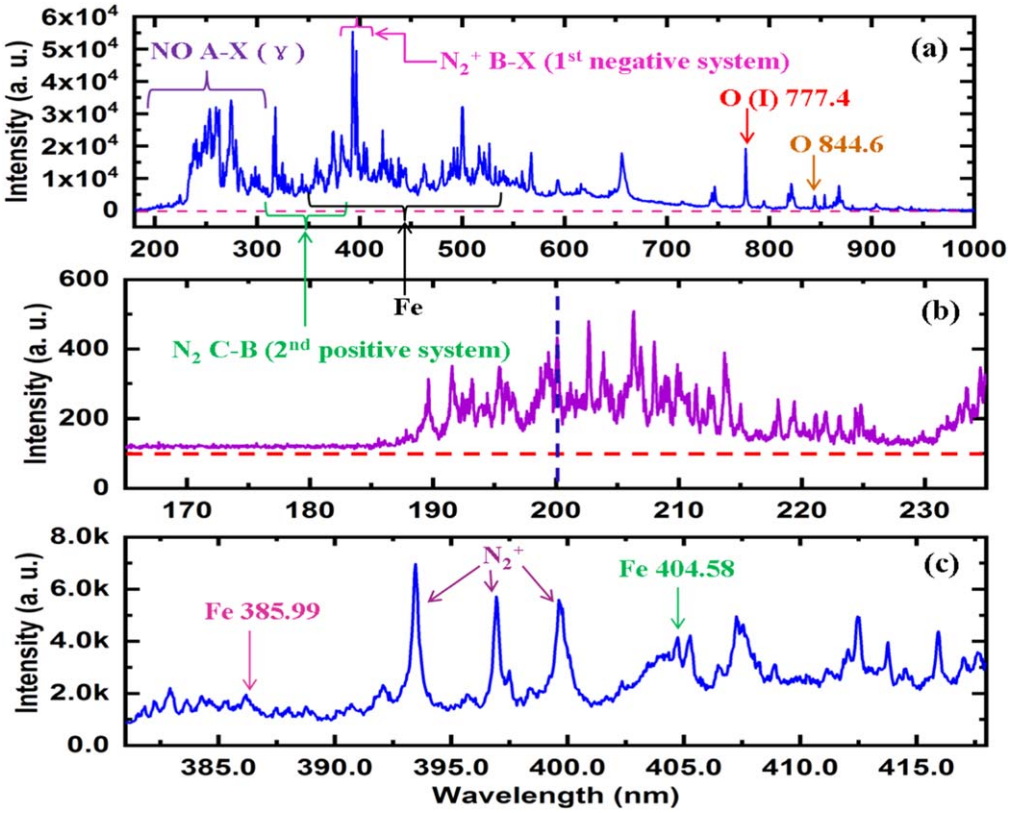

Figure 4. Optical spectrum captured by (a) a fiber spectrometer, (b) and (c) a monochromator, respectively.

As shown in figure 4(b), the VUV photon radiation less than 185 nm is almost a straight line, which indicates that the radiation of spectra are the noise of a spectral device or optical channel. Although we cannot find 98–102.5 nm VUV line spectra, the spectral line in between 90–110 nm radiated by excited N_2 exists to be absorbed by O_2 being used to excite photo ionization. Meanwhile the spectra of 185–235 nm presents really as shown in figure 4(b). Figure 4(c) shows the spectra radiation from 385 nm to 415 nm. We find the spectral line of F_e emissions at 385.99 nm and 404.58 nm, which suggests that the electrodes have taken part in the spark discharge process. We have known that the photo-electron work of iron is 3.9 eV; that is to say, as long as the ultraviolet light with wavelength less than 300 nm irradiates the surface of the iron electrode, photo electrons will escape from the surface of the cathode [28–30].

3.2. High-speed discharge images

Figure 5 shows the high-speed discharge images obtained from the plasma jet in ambient air. The work condition of the ICCD camera is fixed in the interface of camera-controlled software. The time marked in figure 5 is the time when the photo starts to be collected, and the exposure time of each photo is 20 ns. At the time of 1 μs, a bright plasma jet plume generates at the output of the cathode nozzle. From 2 μs to 4 μs, the plasma jet plume only becomes more brightened but seems not to stretch forward. After the time of 5 μs, the plasma jet plume starts to grow up in the direction of jet axis until 10 μs. It is interesting to note that there is a bullet-shaped ionization wave front ahead of plasma jet and along with time the front head becomes bigger. After the time of 40 μs, the plasma bullets look like a mushroom cloud from an atomic bomb explosion. Until 130 μs, the emitted light from the plasma jet plume is too weak to be detected by camera. As shown in figure 5, that is the entire movie frame of one discharge.

At first glance, it is difficult to understand a strange phenomenon that is observed, which is why the plasma jet front is not stretching forward during the time from 1 μs to 5 μs, as shown in figure 5. Observing carefully, we find there always exists the weaker light area ahead of each brightened area. We predict that these weaker light areas are caused by photo ionization. In order to verify this prediction, we can reduce their brightness of high-speed discharge images to one tenth of the normal value, and to do that the weaker light areas shall be brightened clearly. As shown in the left three columns of figure 6, there are exactly the bullet-shaped lightened domains ahead of each plasma jet, at the times of 2 μs, 3 μs, and 4 μs, respectively. During the times from 5 μs to 11 μs, the weaker light area of the plasma jet is still in existence with much weaker intensity. Although the intensity of this ionization is much weaker in comparing with the stronger tail of the plasma jet, it is important to guide the development direction of the plasma bullet [2].

Moreover, we believe these weaker light areas are originated from photo ionization because we know that a large amount of ultraviolet photons with the wavelength shorter

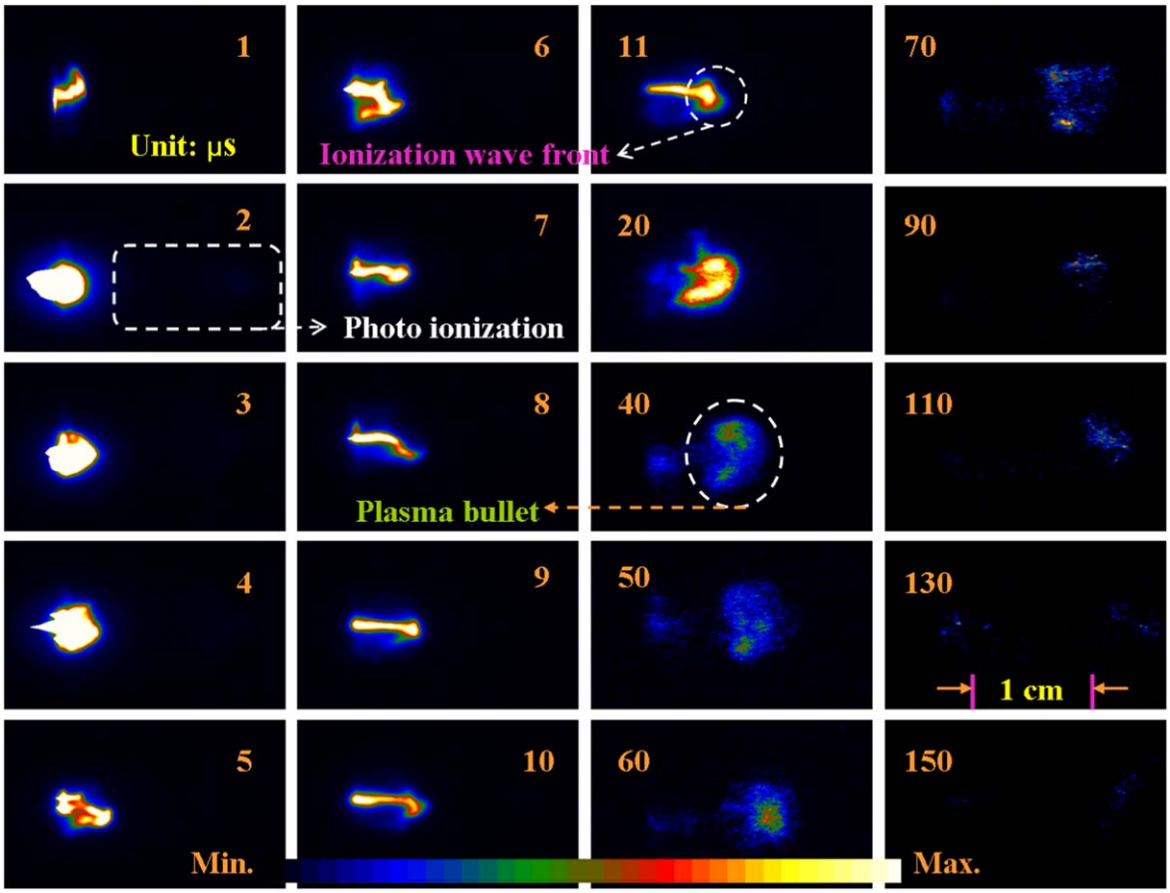

Figure 5. High-speed discharge images obtained from the plasma jet plume in ambient air. The photo images are shown in natural light intensity. The exposure time of 20 ns, the optical gain of 2000 and the time step of 1 μs are applied to the ICCD camera.

than 350 nm have been generated in the air spark discharge, as shown in figure 4. Further speculation is that the high-energy ultraviolet photons are mainly produced in the cavity of the cathode and thereafter radiate out through the hole of the cathode, which can be used to interpret why the bullet-shaped lightened domain (photo ionization) is only generated in the forward region of the plasma jet plume. Furthermore, other discharge experiments have been carried out to verify whether the ionization occurring in the weaker light area is photo ionization or not. We put a piece of quartz sheet (3 mm thick) and a 6 mm thick pork layer respectively, in front of the cathode end of 2 mm. Then the weaker light area is also in existence at the domain of another side of quartz sheet or pork layer. For instance, at the times of 2 μs, 3 μs, and 4 μs respectively, they all have a hemispherical weaker light domain with much weaker light intensity present at the right side of the pork layer, as shown in the right three columns of figure 6. That is to say, the high-energy ultraviolet photons penetrate the light-transmitting medium and then induce the occurrence of photo ionization. In other words, the seed electrons in charge of guiding the propagation of ionization wave front are only originated from photo ionization but not from others. In short, we have observed photo ionization for the first time in the air spark discharges and the bullet-shaped photo ionization wave front guides the development of the proposed plasma jet.

3.3. Laser schlieren images

The following focus is laid on the ionization development process of air spark discharge. The laser schlieren images might help us to understand the process that happens [31–33]. Figure 7 shows laser schlieren images. At the time of 1 μs, one shock wave front and a large sheet of bright spot present. We call this shock wave the 1st shock wave, and the bright spot is photo-enhanced ionization induced by the stronger UV light radiation of spark discharge. Until 2 μs, the 1st shock wave disappears and the plasma jet front attends. About 4 μs, the 2nd shock wave gives birth from the plasma jet front. At the time of 11 μs, the 2nd shock wave starts to separate from the plasma jet and after then it moves forward more quickly than the plasma jet front. Therefore, the lightened plasma jet at the time of 1 μs is not from the plasma that was the blowout from the cavity of the cathode, but might be the ionization generated by photo-enhanced ionization. At the time of 2 μs, the plasma in the cathode cavity is sprayed out and superposes with the plasma jet front generated by photo ionization, which makes the light radiation at the time of 2 μs become stronger abruptly, as shown in figures 5 and 6. In addition, as shown in figure 7, it is interesting to find that the pattern of the plasma jet plume presents as the shape of a bottle gourd (two balls meeting together with a thin waist in the middle) after the time of 30 μs.

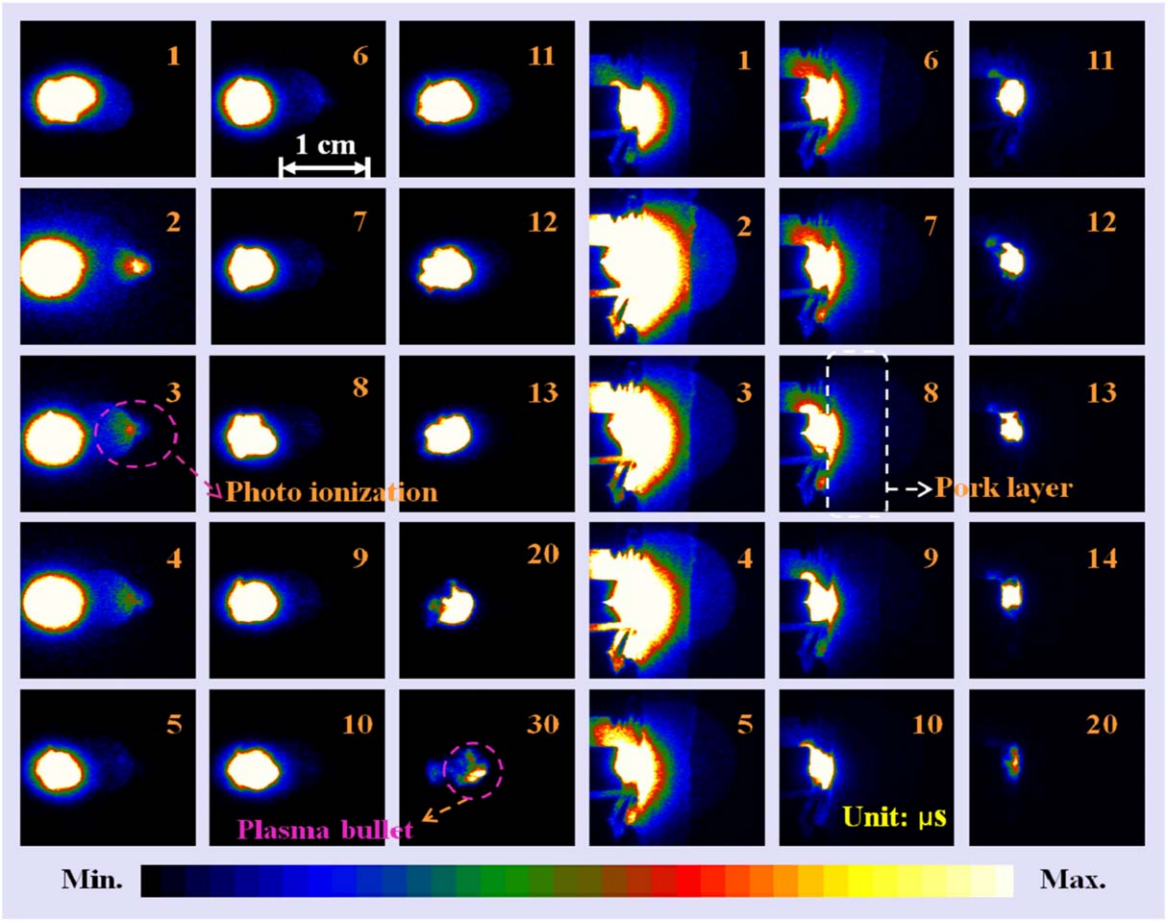

Figure 6. High-speed discharge images captured by ICCD camera. The figures are shown in weak light intensity. The left three columns are the photos from the plasma jet plume in ambient air and the right three columns are the images from the plasma jet plume shot to a 6 mm thick pork layer (2 mm ahead of the cathode end). The exposure time of 20 ns, the optical gain of 2000 and the time step of 1 μs are also used.

According to the propagation of shock waves present in the laser schlieren images in figure 7, the distance of the shock wave front departing from the nozzle can be recorded. Meanwhile the velocity of the shock wave can also be calculated. Figure 8 shows the velocity and distance of the shock wave as time goes on. For its distance from the nozzle, the point at 1 μs is the value of the 1st shock wave while other points are the data of the 2nd shock waves. For the curve of velocity, we only count the numbers of the 2nd shock waves. As shown in figure 8, the speed of propulsion of the shock wave is supersonic and the peak of velocity can approach about 1000 ms^{-1}. It is not until the length of the plasma jet stops growing that the speed of the shock wave front drops to the value of the sound speed in the ambient air (about 340 ms^{-1} at 80 μs approximately). For the point at 1 μs, the distance from the nozzle gets to about 10 mm and thence the velocity of the 1st shock wave front arrives at 10^4 ms^{-1}, which value is already in the range of plasma ionization wave velocity (most of plasma bullet propagates at 10^3–10^6 ms^{-1}) [1–5].

3.4. Temperature measurements

The temperature of the plasma jet is an important factor in applications. The proposed plasma jet is required to be directly touched by the human body; that means it is necessary that the gas temperature of the plasma jet outside of the nozzle is not higher than 50 °C. Figure 9 shows the measurement of the gas temperature of the air plasma jet away from the nozzle. A thermocouple probe is fixed on the bracket of a two-dimensional moving platform. The distance between the probe and the nozzle is manually adjusted, and a value is recorded with a step distance of 1 mm. Due to the slow response of the thermocouple probe, the probe does not move for 10 s each time, and then reads the measured value; Each position we measure three times, and take an average value to reduce random error. The experiment is done under room temperature at about 15 °C. As shown in figure 9, the gas temperature of the plasma jet plume decreases monotonously with the increment of the distance, and the temperature at the nozzle is with the highest value but less than 45 °C. Therefore, the proposed air plasma jet can be used to touch the human body directly without a scalding hazard.

3.5. Discussion on the photo ionization

Addressing more attention to the role of photo ionization in guiding the propagation of plasma bullets, due to the major experimental difficulties, there are no direct photo ionization

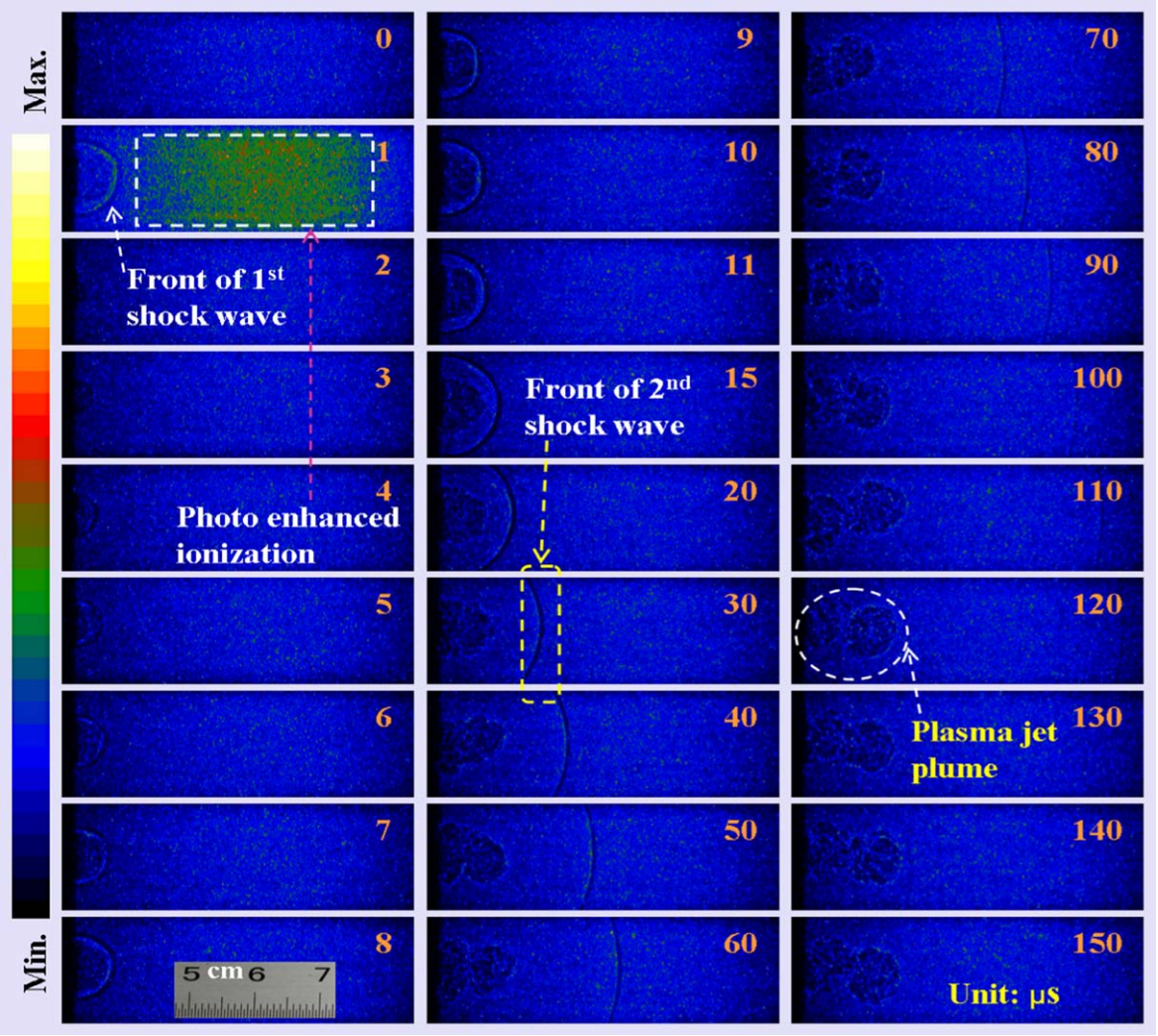

Figure 7. Laser schlieren images taken from the air plasma jet plume in ambient air for showing shock waves. The exposure time of 20 ns, the optical gain of 2000 and the time step of 1 μs are still used.

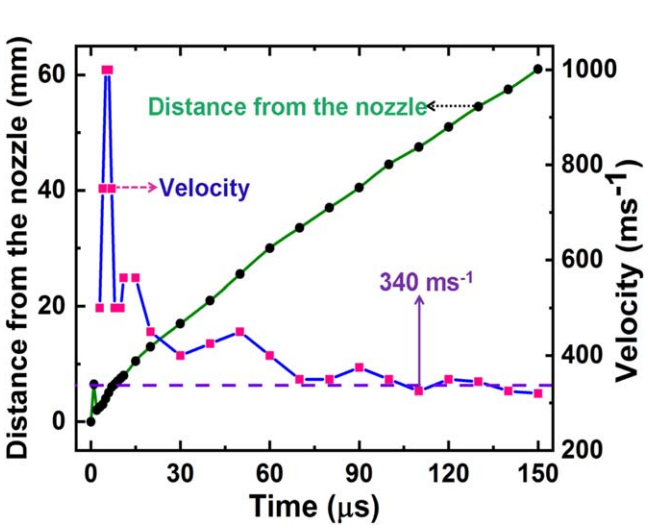

Figure 8. The velocity and distance of the shock wave from the nozzle.

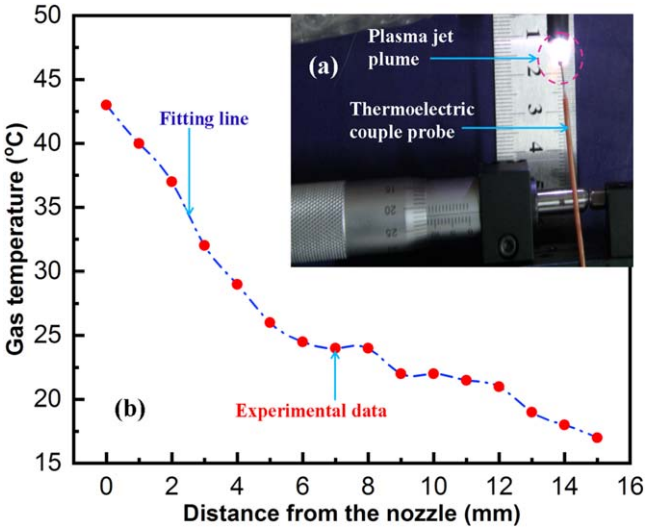

Figure 9. Gas temperature of the air plasma jet plume away from the nozzle.

experiments reported, not to mention the high-speed images attributed to photo ionization. The main reason is that the density of photo electrons of the order of $10^{13}\,\mathrm{m}^{-3}$ is relatively lower for most APPJs [2–5]. While the plasma bullet propagated in a repeatable mode needs a ionization wave front that is with a high seed electron density of the order of $10^{15}\,\mathrm{m}^{-3}$ [2, 34–36]. That is to say the photo electrons only occupy very small share on the total seed electrons in the most of the guided plasma jets. As a result, only photo ionization cannot maintain the existence of ionization wave; photo ionization has taken part in the generation of the plasma bullet, but it is very difficult to distinguish photo electrons from all of the seed electrons, or which ionization is induced by photo ionization. In our experiments, the high-speed images display the propagation of the photo ionization wave front directly. The entire brightened spot at 1 μs and the forward weaker light spots ahead of each over brightened tails during 2–10 μs are all generated by photo ionization, as shown in figures 5–7. Therefore, the photo ionization afforded enough seed electrons that are capable of guiding the propagation of plasma bullets forward.

We continue to discuss in detail whether the plasma bullet in the present air plasma jet is guided by photo ionization or not. At the time of 1 μs, the plasmoid in the cathode cavity is not sprayed out to the nozzle outlet, which is shown clearly in figure 7 (where no dark spot is present). Meanwhile, the plasma jet is generated ahead of the nozzle outlet, as shown in figures 5 and 6. This phenomenon can only be interpreted as that the plasma bullet at 1 μs is excited by photo ionization. The air spark discharge in the cathode cavity can emit a large amount of high-energy photons; these photons pass through the hole of the cathode and project into domains outside the nozzle; thereafter the photo ionization of air takes place to form a plasma jet immediately; next, the plasmoid in the cavity is ejected out of the nozzle and converges with the plasma bullet formed by photo ionization, then the brightness of the subsequent plasma jet plume is greatly enhanced. Therefore, only photo ionization can provide the seed electrons necessary for plasma ionization wave propulsion; thereafter the above all experimental phenomena and processes can be interpreted. However, according to Lu's review report on the propagation of the ionization wave [2], the seed electrons generated by photo ionization are of the order of 10^{13}–$10^{14}\,\mathrm{m}^{-3}$ and the plasma ionization wave that can produce repeatedly needs the density of seed electrons higher than $10^{15}\,\mathrm{m}^{-3}$ for most APPJs. That is to say only photo ionization could not generate the repetitive ionization wave, which contradicts with our experimental findings.

In fact, the plasma density in the spark discharge channel is very over dense. We have calculated the resistance of the spark channel to $R_\mathrm{p} = 0.57\ \Omega$. From R_p, the conductivity σ can be acquired and finally the electron density n_e can be counted [37–39],

$$\sigma = \frac{l_0}{\pi r_0^2 R_\mathrm{p}}, \tag{4}$$

$$n_\mathrm{e} = \frac{\sigma m_\mathrm{e}}{e^2}\gamma_\mathrm{en}, \tag{5}$$

$$\gamma_\mathrm{en} = 1.52 \times 10^7 P[\mathrm{Pa}]\sqrt{T_\mathrm{e}[\mathrm{eV}]}, \tag{6}$$

where l_0 is the length of spark channel and here is 2 mm air gap in the cathode cavity; r_0 is the radius of the spark channel (using the inner radius of ceramic tube of 1 mm); m_e and e are the mass of electron and charge quantity of elementary charge, respectively; P is gas pressure and γ_en is the collision frequency of electrons and neutral particles. Using the electron temperature T_e of 1 eV, $n_\mathrm{e} = 6.01 \times 10^{22}\,\mathrm{m}^{-3}$ can be obtained. This is much stronger discharge and the concentration of nitrogen molecules in the excited state is likely to be higher than this value, if we take the contribution of excited state N_2 produced by multistage photon ionization and photo excitation into account. Here we make a conservative estimation of the density of photo electrons. As long as one-thousandth of the excited state of nitrogen molecules can radiate high-energy photons with the wavelength of 98–102.5 nm, and one-tenth of these high-energy photons pass through the hole of cathode, and one-thousandth of the high-energy photons outside the nozzle can ionize oxygen molecules, the plasma bullet with the electron density of $n_\mathrm{e} = 6.01 \times 10^{15}\,\mathrm{m}^{-3}$ could be successfully generated by the photo ionization only. Actually, the electron density measured by the microwave Rayleigh scattering method [40–42] is of the order of $10^{20}\,\mathrm{m}^{-3}$, and this value is far greater than the required value of $10^{15}\,\mathrm{m}^{-3}$, at the moment of 1 μs. The detailed measurement process has been reported in reference [42].

Moreover, the current photo ionization theory on air discharge assumes that excited N_2 emits radiation with the wavelength of 98–102.5 nm, which can cause ionizing O_2 species. However, the experimental results [43, 44] reported that the propagation behavior of the steamer does not vary much when O_2 concentration is changed dramatically. This intriguing discrepancy is mainly caused by the incomplete pathways of the currently widely accepted photo ionization models. One possible pathway is multistage photon ionization, especially two-photon ionization. Wu *et al* [19, 45] in their work have found that the UV lines at 365 nm radiated by a mercury lamp can decrease the ignition delay time to more than two orders of magnitude, which suggests that the seed electrons used to shorten the ignition delay time are likely produced by multistage photon ionization. In our experiment, there are a lot of short wavelength lines in the measured spectra (as shown in figure 4). Therefore, we believe that multistage photon ionization could also contribute a lot of photo electrons. For most APPJs, only photo ionization cannot maintain the repetitive generation of the ionization wave; the reason is that the maximum electron density can merely reach $10^{20}\ \mathrm{m}^{-3}$ and the photo electrons generated ahead of the ionization wave front are of the order of 10^{13}–$10^{14}\,\mathrm{m}^{-3}$ [1–6]. For the proposed air plasma jet, the electron density in the discharge cavity can get up to $10^{22}\,\mathrm{m}^{-3}$, and the density of photo electrons should be far greater than 10^{15}–$10^{16}\,\mathrm{m}^{-3}$ (the electron density of $10^{20}\,\mathrm{m}^{-3}$ has been measured by the microwave Rayleigh scattering method at the time of 1 μs) [42], which has satisfied the required value for maintaining the continuous propulsion of plasma bullets. Therefore, we have verified that the discharge intensity of the proposed plasma jet is strong enough to produce enough photo

electrons, which further easily ensures the directional propulsion of the ionization waves.

4. Conclusions

In summary, photo ionization has been observed directly in a dc spark air plasma jet generated by the proposed portable cold plasma device. The discharge images captured by an ICCD camera show that the propagation of ionization wave fronts are guided by the photo electrons, which are generated ahead of the plasma bullet. The plasma ionization can take place at another side of the quartz plate or pork layer (6 mm thick), which indicates that the ionization should be attributed to photo ionization. Based on the photo ionization theory and the optical spectrum measurement, the direct photo ionization and multistage photo ionization are the main factors that are in charge of generating the cold air plasma jet plume. Moreover, the laser schlieren images indicate there is propagation of a shock wave along with the plasma bullet. The spark discharge in the cathode cavity is strong enough to produce a large amount of high-energy photons, and the density of photo electrons over the required value that induces the directional propulsion of the plasma bullets, by photo ionization only. The plasma jet plume outside of the nozzle is colder than 320 K and can be touched safely by the human body. In view of the plasma jet plume containing a large amount of active particles, such as NO, O, OH, emitted photons, etc, the proposed portable cold air plasma jet device could be qualified for plasma bio-medicine applications.

Acknowledgments

The authors are grateful for financial support from National Natural Science Foundation of China (Nos. 11575003, 51607003).

References

[1] Lu X *et al* 2019 *Mater. Sci. Eng. R Rep.* **138** 36
[2] Lu X P and Ostrikov K 2018 *Appl. Phys. Rev.* **5** 031102
[3] Lu X *et al* 2016 *Phys. Rep.* **630** 1
[4] Lu X *et al* 2014 *Phys. Rep.* **540** 123
[5] Lu X, Laroussi M and Puech V 2012 *Plasma Sources Sci. Technol.* **21** 034005
[6] Chen Z Q *et al* 2019 *IEEE Trans. Plasma Sci.* **47** 4787
[7] Wu S Q *et al* 2011 *IEEE Trans. Plasma Sci.* **39** 1489
[8] Chen Z Q *et al* 2014 *Plasma Sci. Technol* **16** 329
[9] Chen Z Q *et al* 2013 *IEEE Trans. Plasma Sci.* **41** 1658
[10] Pei X *et al* 2012 *J. Phys. D: Appl. Phys.* **45** 165205
[11] Fridman G *et al* 2008 *Plasma Process. Polym.* **5** 503
[12] Reuter S, Von Woedtke T and Weltmann K D 2018 *J. Phys. D: Appl. Phys.* **51** 233001
[13] Kang S K *et al* 2015 *Plasma Sources Sci. Technol.* **24** 035020
[14] Dobrynin D *et al* 2011 *J. Phys. D: Appl. Phys.* **44** 075201
[15] Dobrynin D, Fridman A and Starikovskiy A Y 2012 *IEEE Trans. Plasma Sci.* **40** 2613
[16] Douat C *et al* 2012 *Plasma Sources Sci. Technol.* **21** 034010
[17] Breden D, Miki K and Raja L L 2012 *Plasma Sources Sci. Technol.* **21** 034011
[18] Xiong Z M and Kushner M J 2012 *Plasma Sources Sci. Technol.* **21** 034001
[19] Wu S *et al* 2014 *Phys. Plasmas* **21** 103508
[20] Chen Z Q *et al* 2018 *Chin. Phys.* B **27** 055202
[21] Li P *et al* 2018 *J. Appl. Phys.* **123** 123302
[22] Chen Z Q *et al* 2017 *J. Appl. Phys.* **122** 093301
[23] Chen Z Q *et al* 2017 *J. Appl. Phys.* **121** 023302
[24] Malik M A 2016 *Plasma Chem. Plasma Process.* **36** 737
[25] Zheleznyak M B, Mnatsakanian A K and Sizykh S V 1982 *High Temp.* **20** 357–62 (in Russian)
[26] Naidis G V 2006 *Plasma Sources Sci. Technol.* **15** 253
[27] Georghiou G E, Morrow R and Metaxas A C 2001 *J. Phys. D: Appl. Phys.* **34** 200
[28] Wang Y *et al* 2016 *J. Anal. At. Spectrom.* **31** 497
[29] Wang Y *et al* 2016 *Plasma Sci. Technol* **18** 1192
[30] Zhu X M *et al* 2009 *J. Phys. D: Appl. Phys.* **42** 142003
[31] Liu R B *et al* 2015 *Sci. China Technol. Sci.* **58** 1949
[32] Zhou Y *et al* 2017 *Sci. China Technol. Sci.* **60** 146
[33] Wang L *et al* 2014 *Sci. China Phys. Mech. Astron.* **57** 2309
[34] Shao T *et al* 2014 *Europhys. Lett.* **107** 65004
[35] Huang B D *et al* 2018 *J. Phys. D: Appl. Phys.* **51** 225202
[36] Huang B D *et al* 2019 *Plasma Sources Sci. Technol.* **28** 095001
[37] Chen Z Q *et al* 2014 *J. Appl. Phys.* **116** 153303
[38] Chen Z Q *et al* 2012 *Plasma Sci. Technol* **14** 754
[39] Chen Z Q *et al* 2012 *Rev. Sci. Inst.* **83** 084701
[40] Shashurin A *et al* 2009 *Appl. Phys. Lett.* **94** 231504
[41] Shashurin A *et al* 2010 *Appl. Phys. Lett.* **96** 171502
[42] Wu J F *et al* 2020 *Acta Phys. Sin.* **69** 075202 (in Chinese)
[43] Wormeester G *et al* 2010 *J. Phys. D: Appl. Phys.* **43** 505201
[44] Nijdam S *et al* 2010 *J. Phys. D: Appl. Phys.* **43** 145204
[45] Wu S Q *et al* 2017 *Plasma Sources Sci. Technol.* **26** 09LT01